Radiative transfer modelling for humidity

Marco Matricardi, Frédéric Chevallier, Graeme Kelly and Jean-Noël Thépaut

European Centre for Medium-Range Weather Forecasts
Reading, UK

Summary

An improved version of the RTTOV fast radiative transfer model used operationally at the European Centre for Medium-Range Weather Forecasts for the assimilation of advanced TIROS operational vertical sounder radiances has been developed. This new model reproduces line-by-line radiances and Jacobians for the surface sensing, water vapour and ozone channels of the advanced TIROS operational vertical sounder with significantly improved accuracy. The profile-dependent predictors used by the improved model to parameterise the atmospheric optical depths are based on the approach followed by RTIASI, the ECMWF fast radiative transfer model for the Infrared Atmospheric Sounding Interferometer.

1. Introduction

Radiances from the Advanced TIROS Operational Vertical Sounder (ATOVS) on the National Oceanic and Atmospheric Administration (NOAA) polar orbiting satellites are used at the European Centre for Medium-Range Weather Forecasts (ECMWF) by assimilating the radiances directly into the four-dimensional variational analysis scheme (Rabier et al. 1998). A prerequisite for exploiting radiance data from satellite sounders is the availability of a fast radiative transfer model (usually called the observation operator) to predict a first guess radiance from the model fields (temperature, water vapour, ozone, surface emissivity and perhaps clouds at a later time) corresponding to every measured radiance. The minimisation procedure involved in 4D-Var requires the computation of the gradient of the cost function (measuring a weighted departure between the observation and the model equivalent) with respect to the atmospheric profile. The radiative transfer model and its adjoint are therefore a key component to enable the assimilation of satellite radiance in a NWP system.

The parameterisation of the transmittances used in RTTOV-5, the fast radiative transfer model currently operational at ECMWF (Saunders et al. 1999), makes the model computationally efficient and in principle should not add significantly to the errors generated by uncertainties in the spectroscopic data used by the line-by-line (LBL) model on which the fast model is based. While for the ATOVS stratospheric temperature sounding channels the model can reproduce LBL model radiances to an accuracy below the instrumental noise, for the surface sensing, ozone and, most importantly, water vapour channels, errors introduced by the parameterisation of the transmittances are above the instrumental noise and can be a significant fraction of the errors introduced by spectroscopic uncertainties in the LBL model (Rizzi et al. 2001). It has also been shown (Garand et al. 2001) that significant differences exist between Jacobians computed using RTTOV-5 and a LBL model. Since the Jacobian is a fundamental quantity in the direct assimilation of satellite radiance in an NWP model (analysis increments will differ if Jacobians differ) it is desirable to improve the accuracy of the operational fast model Jacobians.

The set of predictors developed for RTIASI, the ECMWF fast radiative transfer model for the Infrared Atmospheric Sounding Interferometer (IASI) (Matricardi and Saunders, 1999) was implemented into the RTTOV-5 scheme to improve prediction of the High-Resolution Infra-Red Sounder (HIRS) channels. Results obtained by use of the new predictors demonstrate that a single set of predictors can be used to

accurately reproduce LBL radiances for a wide range of satellite instruments, from the conventional infrared to the microwave sounders. As a result of this, a new version of RTTOV, RTTOV-7, has been jointly developed with Météo France and The Met Office that among the other new features includes the use of the new predictors. The methods that were applied to develop RTTOV-7 are described in section 2. In section 3 the performance of the fast model is described by comparing fast model transmittances and radiances with LBL equivalents. Results of an assimilation experiment are described in section 4. Conclusions are given in section 5.

2. The fast radiative transfer model for TOVS

2.1. General description of the model

For a detailed description of RTTOV, the reader can refer to Saunders et al. (1999). Only the main components of the fast transmittance scheme are discussed here.

The fast transmittance stage of RTTOV-7 is based on algorithms that have been developed over the years for a number of different satellite instruments (McMillin et al. 1979, Susskind et al. 1983, Eyre 1991, Hannon et al. 1996, Matricardi and Saunders 1999). For a given input atmospheric profile (temperature, water vapour, and ozone volume mixing ratio) and surface variables (emissivity, pressure, temperature, skin temperature), the computation of the convolved level-to-space transmittance $\hat{\tau}_{j,\tilde{\nu}^*}$ or convolved level-to-space optical depth $\hat{\sigma}_{j,\tilde{\nu}^*}$ ($\hat{\tau}_{j,\tilde{\nu}^*} = \exp-[\hat{\sigma}_{j,\tilde{\nu}^*}]$) is performed by the fast transmittance model and is the essence of RTTOV-7. The computation of the optical depth for the layer from pressure level *j* to space along a path at angle θ involves a polynomial with terms that are functions of temperature, absorber amount, pressure and viewing angle. The convolved optical depth at wave number $\tilde{\nu}^*$ from level j to space can be written as:

$$\hat{\sigma}_{j,\tilde{\nu}^*} = 0 \quad j = 1 \tag{1}$$

$$\hat{\sigma}_{j,\tilde{\nu}^*} = \hat{\sigma}_{j-1,\tilde{\nu}^*} + \sum_{k=1}^{M} a_{j-1,\tilde{\nu}^*,k} \; X_{k,j-1} \quad j = 2,44 \tag{2}$$

where *M* is the number of predictors and the functions $X_{k,j}$ constitute the profile-dependent predictors of the fast transmittance model. To compute the expansion coefficients $a_{j,\tilde{\nu}^*,k}$ (sometimes referred to as fast transmittance coefficients), a set of diverse atmospheric profiles is used to compute, for each profile and for several viewing angles, accurate LBL transmittances for each level defined in the atmospheric pressure layer grid. Line-by-line transmittances were here computed using GENLN2 (Edwards, 1992), a general purpose LBL atmospheric transmittance and radiance model. The convolved level-to-space transmittances $\hat{\tau}_{j,\tilde{\nu}^*}$ are then used to compute the $a_{j,\tilde{\nu}^*,k}$ coefficients by linear regression of $\hat{\sigma}_{j,\tilde{\nu}^*} - \hat{\sigma}_{j-1,\tilde{\nu}^*}$, or equivalently

$$-\ln\left(\frac{\hat{\tau}_{j,\tilde{\nu}^*}}{\hat{\tau}_{j-1,\tilde{\nu}^*}}\right) \tag{3}$$

versus the predictor values calculated from the profile variables for each profile at each viewing angle.

For each gas allowed to vary, the profiles used to compute the database of LBL transmittances are chosen to represent the range of variations in temperature and absorber amount found in the real atmosphere. In this paper only H_2O and O_3 are allowed to vary, the others are held constant and will be referred to as fixed. The

water vapour and fixed gas fast transmittance coefficients were derived by use of a training set of 42 profiles. To derive the regression coefficients for ozone, 33 profiles were used.

Once the LBL transmittances were integrated over the channel spectral responses, they were used to compute three sets of regression coefficients because the fast model treats separately the absorption by the fixed gases, water vapour, and ozone. Since the convolution of the transmittance of all the gases differs from the product of the transmittance of the single gases convolved individually, the monochromatic transmittance approximation

$$\hat{\tau}^{tot}_{\tilde{\nu}^*,j} = \hat{\tau}^{fix}_{\tilde{\nu}^*,j} \quad \hat{\tau}^{wv}_{\tilde{\nu}^*,j} \quad \hat{\tau}^{oz}_{\tilde{\nu}^*,j} \tag{4}$$

where $\hat{\tau}^{tot}_{\tilde{\nu}^*,j}$ is the convolved transmittance of all the gases and $\hat{\tau}^{fix}_{\tilde{\nu}^*,j}$, $\hat{\tau}^{wv}_{\tilde{\nu}^*,j}$, and $\hat{\tau}^{oz}_{\tilde{\nu}^*,j}$ are the transmittances of the single gases convolved individually, might not be accurate because, for example, absorption by water vapour is not totally uncorrelated with absorption by the fixed gases. To reduce the errors introduced by separation of the gas transmittances after convolution, the total model transmittance is written as:

$$\hat{\tau}^{tot}_{\tilde{\nu}^*,j} = \hat{\tau}^{fix}_{\tilde{\nu}^*,j} \quad \frac{\hat{\tau}^{fix+wv}_{\tilde{\nu}^*,j}}{\hat{\tau}^{fix}_{\tilde{\nu}^*,j}} \quad \frac{\hat{\tau}^{fix+wv+oz}_{\tilde{\nu}^*,j}}{\hat{\tau}^{f+wv}_{\tilde{\nu}^*,j}} \tag{5}$$

where the superscripts denote what was included in the LBL computations and the three terms on the right hand side of Eq. (6) are what is predicted by the fast model. Since all the terms but $\hat{\tau}^{fix+wv+oz}_{\tilde{\nu}^*,j}$ cancel, the correct total convolved transmittance is left.

2.2. The fast transmittance model

The functional dependence of the predictors $X_{j,k}$ used to parameterise the optical depth $\hat{\sigma}_{j,\tilde{\nu}^*}$ depends mainly on factors such as the absorbing gas, spectral response function and spectral region although the order in which the gases are separated out (Eq. 5) and the layer thickness can also be important. The model predictors used in this paper are listed in Table 1 whereas the profile variables are defined in Table2.

Within the framework of a linear regression method, the great variability between extreme profiles makes the regression prone to numerical instabilities and thus difficulties in calculating the coefficients can arise if the predictors are allowed to vary too much. To avoid these difficulties predictors in this paper are defined by taking the ratio with respect to the values for a reference profile (see table 2).

Since most of the absorption in the temperature sounding channels is due to gases whose concentration is held fixed, transmittances for these channels are less difficult to model in that for a given viewing angle the transmittance depends only on the temperature profile. For water vapour and ozone sounding channels the variation in absorber amount has to be taken into account. The fast transmittance model predicts the polychromatic transmittance defined in Eq. 4. One can give a model to compute transmittances based on the assumption that the basic behaviour of the quantity defined in Eq.2 is that of the layer optical depth for a gas in a homogeneous layer at pressure p(l), temperature T(l) an absorber amount n(l). A set of basic predictors can then be defined based on simple functions of the viewing angle and of the profile variables (all defined in table 2) in the layer j, $T_r(j), W_r(j), O_r(j)$ and $\delta T(j)$. One can expect the layer optical depth to be proportional to n for weak absorption and $\sqrt{n}$ for strong absorption (Goody and Yung, 1989). The

absorption due to the combined effect of weak and strong lines can be obtained using an intermediate value of the exponent. This was accounted for by introducing a term proportional to $\sqrt[4]{n}$. Values of the exponent greater than 1 can be introduced to account for effects of higher order. For the variable species the slowly varying dependence on temperature was modelled by scaling the terms proportional to n and $\sqrt{n}$ with a $\delta T(j)$ factor. For water vapour only it was found effective to introduce a $|\delta T(j)|\delta T(j)$ factor to scale the term proportional to n. The angular dependence was addressed by scaling the layer amount through the secant of the viewing angle. As discussed above, for a fixed viewing angle the transmittance for the temperature channels depends only on the temperature profile. For these channels the most basic predictors

Predictor	Fixed gases	Water vapour	Ozone
$X_{j,1}$	$sec(\theta)$	$sec^2(\theta)W_r^2(j)$	$sec(\theta)O_r(j)$
$X_{j,2}$	$sec^2(\theta)$	$(sec(\theta)W_w(j))^2$	$\sqrt{sec(\theta)O_r(j)}$
$X_{j,3}$	$sec(\theta)T_r(j)$	$(sec(\theta)W_w(j))^4$	$sec(\theta)O_r(j)\delta T(j)$
$X_{j,4}$	$sec(\theta)T_r^2(j)$	$sec(\theta)W_r(j)\delta T(j)$	$(sec(\theta)O_r(j))^2$
$X_{j,5}$	$T_r(j)$	$\sqrt{sec(\theta)W_r(j)}$	$\sqrt{sec(\theta)O_r(j)}\ \delta T(j)$
$X_{j,6}$	$T_r^2(j)$	$\sqrt[4]{sec(\theta)W_r(j)}$	$sec(\theta)O_r(j)^2O_w(j)$
$X_{j,7}$	$sec(\theta)T_w(j)$	$sec(\theta)W_r(j)$	$\frac{O_r(j)}{O_w(j)}\sqrt{sec(\theta)O_r(j)}$
$X_{j,8}$	$sec(\theta)\frac{T_w(j)}{T_r(j)}$	$(sec(\theta)W_r(j))^3$	$sec(\theta)O_r(j)O_w(j)$
$X_{j,9}$	$\sqrt{sec(\theta)}$	$(sec(\theta)W_r(j))^4$	$O_r(j)sec(\theta)\sqrt{(O_w(j)sec(\theta)}$
$X_{j,10}$	$\sqrt{sec(\theta)}\ \sqrt[4]{T_w(j)}$	$sec(\theta)W_r(j)\delta T(j)\lvert\delta T(j)\rvert$	$sec(\theta)O_w(j)$
$X_{j,11}$	0	$(\sqrt{sec(\theta)W_r(j)})\delta T(j)$	$(sec(\theta)O_w(j))^2$
$X_{j,12}$	0	$\frac{(sec(\theta)W_r(j))^2}{W_w}$	0
$X_{j,13}$	0	$\frac{\sqrt{(sec(\theta)W_r(j)}W_r(j)}{W_w(j)}$	0
$X_{j,14}$	0	$sec(\theta)\frac{W_r^2(j)}{T_r(j)}$	0
$X_{j,15}$	0	$sec(\theta)\frac{W_r^2(j)}{T_r^4(j)}$	0

Table 1. Predictors used by RTTOV-7 for Fixed Gases, Water vapour and ozone.

are drawn on the ratio $T_r(j)$. First and second order terms were included. The inclusion of terms that depend only on the viewing angle had also to be envisaged since the effect of a variable viewing angle is to slightly alter and to impart an offset to the curve that represents the variation of optical depth with temperature. For

water vapour the contribution of the continuum type absorption is of particular importance. The self-continuum contributes to absorption for most of the water vapour infrared channels and is predominant in the window regions. It displays a dependence on the inverse of the temperature and is proportional to the square of water amount. The foreign-continuum is only important at wave numbers greater than 1250 cm-1. It displays a weaker dependence on temperature than the self-continuum and is linearly proportional to the water amount. Given the particular importance for window channels, the self-continuum was included in the water model (predictors $X_{14,j}$ and $X_{15,j}$ in table 1). This is an improvement to the approach followed in RTIASI where no predictors for the continuum were included. Since we are predicting polychromatic transmittances, adjustment terms must be included to extend the validity of the model from monochromatic to polychromatic transmittances. In fact account must be taken for the dependence of the layer transmittance on the properties of the atmosphere above the layer. Despite the fact that Eq. 3 reduces this dependence, the layer transmittance for two profiles having the same layer temperature but different temperature profiles over the actual layer will nevertheless differ in that the profile with greater optical depth above the layer will have smaller optical depth within the layer. This effect can be modelled by introducing predictors representative of the effective temperature and species column density above the layer (Fleming and McMillin 1977). Predictors, $T_w(j), W_w(j)$ and $O_w(j)$ in Table 2 can then be used. The relation between these predictors and the optical properties of the gas is not obvious (for example the different form of the predictors used for the ozone and water model partly reflects the different order in which the gases are separated out in Eq. (5)) and the final form used in this paper was largely derived empirically.

$$T(l) = [T^{profile}(l+1) + T^{profile}(l)] / 2 \qquad T^*(l) = [T^{reference}(l+1) + T^{reference}(l)] / 2$$

$$W(l) = [W^{profile}(l+1) + W^{profile}(l)] / 2 \qquad W^*(l) = [W^{reference}(l+1) + W^{reference}(l)] / 2$$

$$O(l) = [O^{profile}(l+1) + O^{profile}(l)] / 2 \qquad O^*(l) = [O^{reference}(l+1) + O^{reference}(l)] / 2$$

$$T_r(l) = T(l) / T^*(l) \qquad \delta T(l) = T(l) - T^*(l) \qquad W_r(l) = W(l) / W^*(l)$$

$$O_r(l) = O(l) / O^*(l)$$

$$T_w(l) = \sum_{i=2}^{l} P(i) [P(i) - P(i-1)] T_r(i-1)$$

$$W_w(l) = \{\sum_{i=1}^{l} P(i) [P(i) - P(i-1)] W(i)\} / \{\sum_{i=1}^{l} P(i) [P(i) - P(i-1)] W^*(i)\}$$

$$O_w(l) = \{\sum_{i=1}^{l} P(i) [P(i) - P(i-1)] O(i)\} / \{\sum_{i=1}^{l} P(i) [P(i) - P(i-1)] O^*(j)\}$$

The $Pres(l)$'s are the values of the pressure at each level. $T^{profile}(l), W^{profile}(l)$ and $O^{profile}(l)$ are the temperature, water vapour mixing ratio and ozone mixing ratio profiles. $T^{reference}(l)$, $W^{reference}(l)$ and $O^{reference}(l)$ are corresponding reference profiles. For these variables *l* refers to the *l*th level; otherwise *l* is the *l*th layer, i.e.the layer below the *l*th level. Note that we take $P(0) = 2P(1) - P(2)$ and $T_w(1) = 0$.

Table 2. Definition of profile variables used in predictors defined in Table1.

3. Performance of the fast model for simulations of ATOVS radiances

The accuracy of the fast model can be assessed by a comparison of the transmittances and radiances computed by the fast model with the corresponding values from LBL models in different ways. Firstly the fast model transmittance profiles and top of the atmosphere radiances computed for the dependent set of profiles used to train the fast model can be compared with the LBL model equivalents to determine the accuracy of the fast model itself. Secondly a set of profiles independent of the regression coefficients can be

used to allow uncertainties from different type of profiles to be included. Thirdly an independent set of profiles can be used to validate the fast model radiances with a different LBL model to allow spectroscopic and other uncertainties to be included in the validation.

The comparison of transmittances is more useful to understand how the model performs and to see where it needs to be improved, but the comparison of radiances is the most important as the radiances are what will be used. The analysis of the results discussed below concentrates on the error of the RTTOV-7 and RTTOV-5 in terms of the bias, standard deviation and root mean square (rms) of the radiance and transmittance differences between the fast and LBL radiative transfer models.

3.1. Results for the dependent set of profiles

A comparison was made for the channels of the HIRS instruments by comparing the operational and improved fast model transmittances and radiances to the LBL model equivalents. The 43-profile set was used for water vapour and fixed gas transmittances whereas the 34-profile set was used for ozone. Comparisons were made for six viewing angles from 0° to 64°. Results are given for the HIRS channels of NOAA-16. They can be generalised to the HIRS channels of NOAA-14 and NOAA-15 since very slight differences were observed. The computation of the difference between fast model and LBL computed NOAA-14 HIRS (1-19) level-to-space transmittances show a significant and universal improvement when the new model is used. For both operational and improved fast model the bias is generally less than the standard deviation. Best results are for those channels where the absorption is mostly due to fixed gases. Water vapour channels are still the more difficult to model. Scores are improved at all pressure levels and in absolute terms they are most dramatic for channels 8 through 12. This is displayed in Figs. 1 and 2 where the rms of the difference between fast model and LBL computed transmittances is shown for the operational and improved model respectively.

Maximum errors are found near the peaks of the weighting functions. At some pressure levels the rms error for the water vapour channels has been reduced by an order of magnitude. For the ozone and window channel a typical five-fold reduction of the rms error has been achieved.

The ability of the fast model to reproduce the LBL radiances in terms of the bias and standard deviation of the difference between the fast model and LBL computed radiances has also been evaluated. Errors in units of equivalent black body brightness temperature were computed by using the fast model transmittances as compared with those computed by using the LBL transmittances in the radiative transfer equation. Radiances for all 6 viewing angles are included in the statistics. For HIRS channels 9 the model simulates only the ozone transmittance. For this channel water vapour and fixed gas transmittances are taken to be the LBL ones. For the other channels transmittances for a constant climatological profile are used for ozone. Results are discussed for the operational and improved model. For both models, biases are typically less than the standard deviation. However, for the operational model, channel 12 displays a bias that is a significant fraction of the standard deviation. The improved model is virtually unbiased to the LBL. Standard deviations for the temperature sounding channels are marginally improved (for the operational model errors were already well below the noise). A dramatic reduction of the error has been achieved for the other channels. For the window channels HIRS-8 and HIRS-19 the standard deviation has been reduced by an order of magnitude. For the lower tropospheric water vapour channels HIRS-10 and HIRS-11 and for the ozone channel HIRS-9 a five-fold reduction of the standard deviation has been achieved. Note that the rms error for the HIRS-12 upper tropospheric water vapour channel has been reduced from 0.7K to 0.1K. These results are depicted at a glance in Fig. 3 where the rms error for the operational and improved model is shown for the HIRS channels of NOAA-16. Slightly different values of the score are observed for the other platforms but this can be attributed to modification of the spectral response functions.

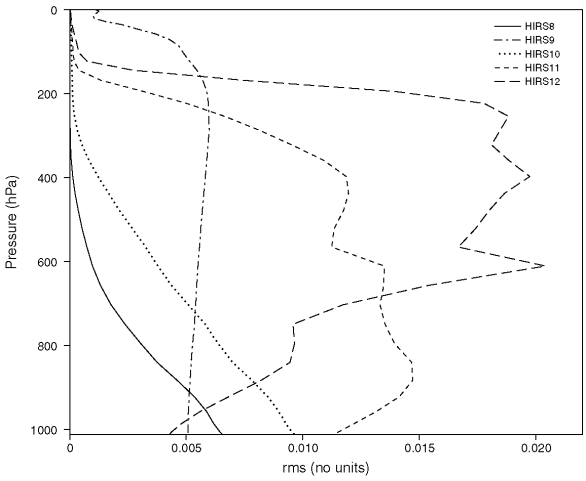

Figure 1. Root mean square of the difference between RTTOV-5 and GENLN2 HIRS channels 8, 9, 10, 11 and 12 layer to top of atmosphere transmittances for NOAA-14 for the profiles used to train the fast model and 6 viewing angles.

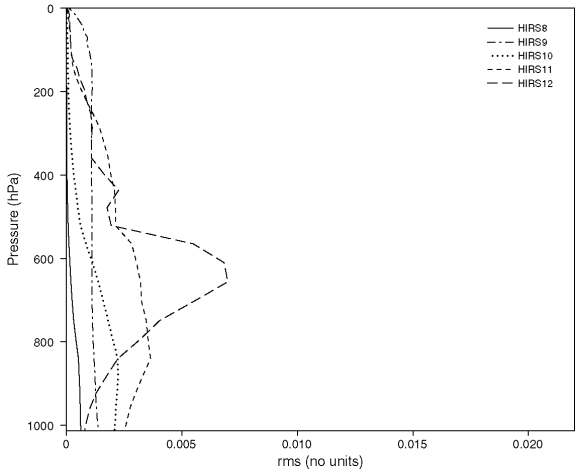

Figure 2. Root mean square of the difference between RTTOV-7 and GENLN2 HIRS channels 8, 9, 10, 11 and 12 layer to top of atmosphere transmittances for NOAA-14 for the profiles used to train the fast model and 6 viewing angles.

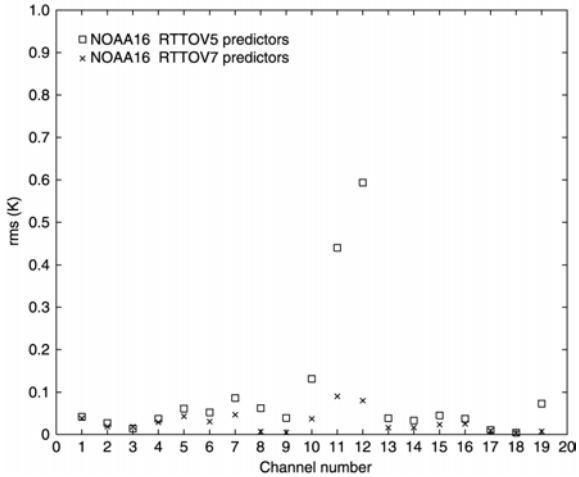

Figure 3. Root mean square of the difference between fast model and GENLN2 computed brightness temperatures for 43 diverse water vapour profiles and six viewing angles. Results are shown for RTTOV-5 and RTTOV-7. The HIRS channels of NOAA-16 are plotted.

For the improved model the signal-to-noise ratio (obtained as the ratio of the rms error in radiance units to the instrument radiance noise) is significantly below 1 for all channels. For the operational model the signal

exceeds the noise for channels HIRS-9, HIRS-10 and HIRS-19 with the same quantity being very close to 1 for channels HIRS-8 and HIRS-11.

3.2. Results for the independent set of profiles

Results for the transmittances of ATOVS channels show that the use of the independent profiles results in a degradation of the scores for both operational and improved fast model. The improved fast model is again performing better than the operational one. As for the dependent set case, improvements were made at all pressure levels. Figures given in section 3(a) regarding the reduction of the rms error made at the various pressure levels are still valid. Note that the relative variation of the standard deviation is roughly the same for both models whereas the relative variation of the bias is larger for the improved model. In fact for this model the bias is now a significant fraction of the standard deviation (but it is still much lower than the operational model bias). For example channel HIRS-9 displays and absolute bias as large as the standard deviation.

A look at the results in terms of brightness temperature differences shows that increments to the values obtained for the dependent set case are in general larger for the operational model. To note is the significantly better accuracy achieved by use of the new predictors for the ozone channel HIRS-9, the window channels HIRS-8 and HIRS-19 and the water vapour channels HIRS-10, HIRS-11 and HIRS-12. In particular for the water vapour channels HIRS-11 and HIRS-12 the standard deviation has been reduced six-fold. For the improved model the signal-to-noise ratio is still significantly below one for all channels. Channels HIRS-8, HIRS-9, HIRS-10, HIRS-11 and HIRS-19 display a signal-to-noise ration larger than 1 when the operational predictors are used.

In general the introduction of uncertainties from the use of different type profiles has not resulted in a dramatic degradation of the performance of the improved model. Errors are still less than 0.13K (results are tabulated in detail in Matricardi et al. 2001) and most importantly they are well below those introduced in the LBL computations by uncertainties in the spectroscopic data. Errors introduced by the parameterisation used in the operational model can instead add significantly to the latter. Note that the improved predictors can be used to reproduce radiances for all the microwave instruments supported by RTTOV-5 to accuracy that is better or at the same level as the one that can be achieved by use of dedicated predictors in RTTOV-5.

3.3. Results for the independent LBL model

The original set of 13766 sampled profiles (reduced to 8978 because profiles with surface pressure less than 950 hPa were excluded) used to derive the 117 independent profiles was used to compare fast model radiances with radiances computed using Synsatrad, a radiative transfer model developed at EUMETSAT (Tjemkes and Schmetz 1997). Synsatrad is based on the radiance sampling method developed by Sneden et al. (1975) and can reproduce LBL radiances to 1-2 % accuracy. For the fixed gases the concentrations were the same used in RTTOV-7. In this validation one allows for several uncertainties to be included in the validation. Typically, uncertainties result from the use of different types of profiles, from different forward model mechanics and from different spectroscopy used in the LBL computations. Results for this exercise are given in Table 3 where the statistics of the difference between fast model and Synsatrad generated radiances is shown for both the operational and improved fast models. Errors were computed for the 8978 profiles described above. Only radiances for the nadir looking case were generated. Spectral response functions for the channels HIRS-8, HIRS-9, HIRS10, HIRS-11 and HIRS-12 of NOAA-14 were considered.

NOAA-14 Channel Number	Operational model				Improved Model			
	Bias (K)	Sdev (K)	Rms (K)	Max Value (K)	Bias (K)	Sdev (K)	Rms (K)	Max Value (K)
8	-0.156	0.107	0.189	0.942	-0.077	0.029	0.082	0.203
9	0.324	0.258	0.414	1.969	0.078	0.153	0.171	1.991
10	-0.055	0.207	0.214	1.001	0.112	0.072	0.133	0.458
11	0.396	0.517	0.652	1.841	0.113	0.103	0.153	0.526
12	0.184	0.858	0.878	5.252	-0.261	0.118	0.287	1.410

Table 3. Statistics of the difference between fast model and Synstrad generated radiances in HIRS channels for the 8978 profile independent set

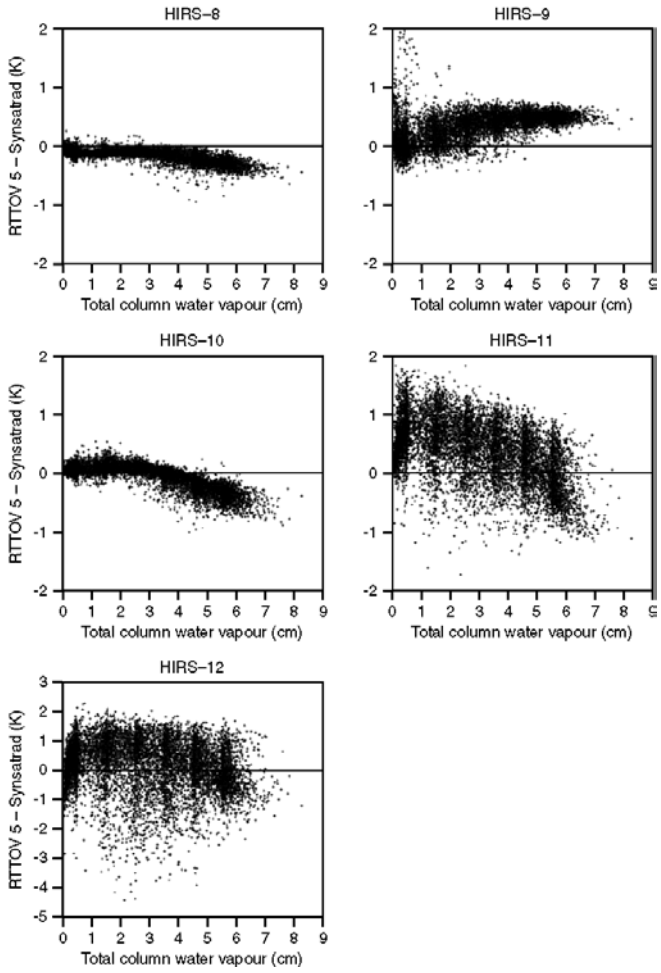

Figure 4. Difference between RTTOV-5 and Synsatrad computed brightness temperatures for 8987 independent profiles for the channels HIRS-8, HIRS-9, HIRS-10, HIRS-11 and HIRS-12 of NOAA-14.

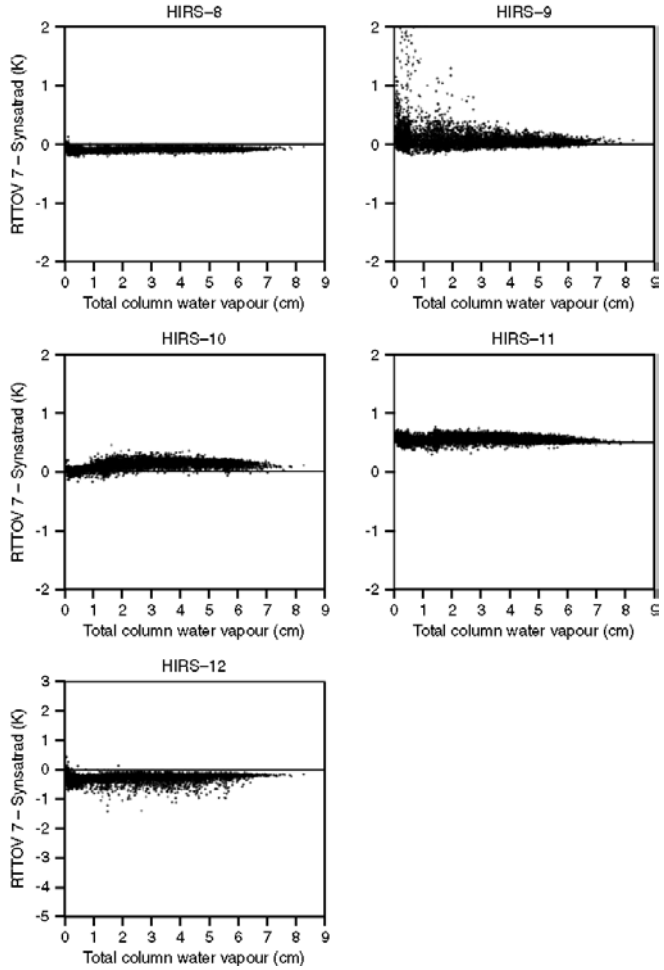

Figure 5. Difference between RTTOV-7 and Synsatrad computed brightness temperatures for 8987 independent profiles for the channels HIRS-8, HIRS-9, HIRS-10, HIRS-11 and HIRS-12 of NOAA-14.

For the channels included in this exercise, results are very similar to those obtained when only uncertainties from different types of profiles were included in the comparison. This means that differences are likely to be dominated by errors in the fast transmittance scheme with differences between the two LBL models (GENLN2 and Synsatrad) playing a less important role. For the improved model standard deviations are in general less than or of the same order as the biases. For channel HIRS-12 a larger bias in observed because of the approximation introduced in the integration of the radiative transfer equation in RTTOV-7 (see Matricardi et al. 2001). For the operational model the standard deviations are typically larger than (for channel HIRS-12 significantly larger) or of the same order as the biases. The use of the new predictors results in a 3-to 4-fold reduction of the rms error. Maximum errors are also significantly reduced. For example the maximum error for channels HIRS-12 has been reduced from to 5.2K to 1.4K. Also to be noted is the performance for the window channel HIRS-8 that with the new predictors displays a maximum error of 0.2K to be compared to 0.94 K obtained with the old predictors. The behaviour of HIRS-9 has yet to be fully understood since the maximum error for the operational and improved fast model is virtually the same although the overall performance for the improved model is significantly better. Maximum errors for this channel are found for very dry and cold profiles.

A major negative feature of the operational fast model that has been corrected by the improved model is the dependence of the error on air mass type. This is illustrated in Figs. 8 and 9 where the error is plotted with the total water content in the profile.

For the operational fast model the error steadily increases with the total water content and is most dramatic in channel HIRS-11 although is clearly visible also for the other channels. This should be compared with the behaviour of the improved model that displays no marked dependence of the error on the air mass type. Errors for this model are randomly distributed. Biases are likely to be due differences between LBL models. The same behaviour (if not worse) is displayed when the error is plotted with the surface temperature or the latitude: the warmer and moister the profile, the larger the error for the operational model.

3.4. Comparison of Jacobians

As stated in the introduction, emphasis should put in the validation of fast model Jacobians since this is a fundamental quantity in the direct assimilation of satellite radiance in a NWP model. In this paper fast model Jacobians were compared to LBL generated Jacobians for the profiles selected in the study of Garand et al. (2001). The GENLN2 Jacobians (obtained by the perturbation method) computed in Garand et al. (2001) were compared to the analytical Jacobians generated by the operational and improved fast model. The quality of fit measure, *M*, defined as

$$M = 100 \sqrt{\frac{\sum_{i=1}^{N} (J_{m,i} - J_{r,i})^2}{\sum_{i=1}^{N} J_{r,i}^2}} \tag{10}$$

where J_m and J_r are the model and reference Jacobian respectively and the sum is over the number of levels, *N*, was computed for five atmospheric profiles (independent of the regression coefficients) and for a selected number of HIRS channels of the NOAA-14 platform. Results for temperature, ozone and water vapour Jacobians are tabulated in Table 4.

Among the profiles used in Garand et al., profiles with number from 7 to 18 are ranked by increasing mean atmospheric temperature, profiles 19-30 are ranked by increasing integrated water vapour and profiles 31-42 by increasing total ozone. Note that if the maximum value of the Jacobian is less than 0.005, no result is given since in that case the value of *M* is meaningless. The first noticeable feature is that for most of the considered cases the quality of fit for the improved model is at a level typical among LBL models ($M \leq 5$). For the temperature sounding channels HIRS-2, HIRS-5 and HRS-15 both models are able to reproduce the LBL temperature Jacobian to a high degree of accuracy ($M \leq 5$), the improved model performing better than the operational one for channels HIRS-5 and HIRS-15, slightly worse for channel HIRS-2. For the ozone channel HIRS-9 scores are significantly better when the improved model is used. The quality of fit for the temperature and ozone Jacobian has been dramatically improved ($M \leq 9.8$), in fact for most of the cases the quality of the fit obtained with the operational model is to be considered fair to marginal ($15 \leq M \leq 25$). Because of the presence of ozone absorption lines, the ozone Jacobian is given for channel HIRS-5 as well. Despite the significantly better quality of the fit, the values of *M* are unusually high for the improved model. This can be partly explained by the fact that the sensitivity to ozone perturbation for this channel is very low and the maximum value of the Jacobian approaches the threshold value quoted above. For the water vapour channels HIRS-10, HIRS-11 and HIRS-12 the temperature and water vapour Jacobians computed using the improved model have the right shape and amplitude and peak at the right height. This results in very low values of the quality of fit measure *M* that never exceeds 8.7 and is for most of the cases smaller than 5 making the fast model Jacobians remarkably close to the LBL ones. Conversely the Jacobians generated by the operational model differ from the LBL ones in amplitude and shape and to some degree the peak position resulting in higher values of *M* that can be as big as 20.

Operational Model

Profile	T H-2	T H-5	O_3 H-5	T H-9	H_2O H-9	O_3 H-9	T H-10	H_2O H-10	T H-11	H_2O H-11	T H-12	H_2O H-12	T H-15
6	2.3	4.1	23.4	17.8	7.9	11.2	8.7	7.1	9.5	12.2	7.7	17.2	2.7
18	2.4	2.7	22.0	27.0	12.2	23.2	5.8	18.9	4.7	16.5	12.2	20.2	2.7
19	2.7	4.5	-----	8.7	-----	19.8	6.3	-----	12.6	10.0	13.5	16.6	3.4
30	2.4	4.2	26.8	10.4	3.1	25.0	8.8	11.5	7.8	17.0	18.5	13.4	2.7
31	2.7	3.9	-----	11.2	-----	9.7	-----	-----	9.5	15.8	10.2	18.0	4.4

Improved Model

Profile	T H-2	T H-5	O3 H-5	T H-9	H2O H-9	O3 H-9	T H-10	H2O H-10	T H-11	H2O H-11	T H-12	H2O H-12	T H-15
6	2.7	2.5	15.2	7.2	3.1	4.6	6.5	3.0	3.1	3.6	1.5	2.0	2.3
18	2.7	2.7	8.4	8.7	1.6	5.2	3.9	3.7	2.1	3.2	3.8	4.2	2.3
19	2.9	2.4	-----	2.7	-----	5.9	6.4	-----	3.6	8.7	2.9	4.6	3.2
30	2.7	2.3	8.3	4.3	1.7	5.8	2.7	2.8	3.0	6.4	7.0	6.8	2.1
31	3.1	2.5	-----	4.6	-----	9.8	-----	-----	3.21	7.5	2.2	6.0	4.3

Table 4. Quality of fit measure F (no units) for temperature (T), ozone (O_3) or water vapour (H_2O) Jacobians for 5 independent atmospheric profiles in selected HIRS channels. Reference line-by-line Jacobians were obtained using GENLN2.

4. Evaluation of the new RT model in assimilation mode

Two twin assimilation experiments have been run for three weeks between 12 November 2000 and 5 December 2000, the only difference between the two being the new RTTOV model used as observation operator in the analysis. The assimilation system used in the two experiments is a 3D-Var system based on the ECMWF Re-Analysis (ERA-40) configuration. This choice was driven by computing time and convenience considerations. The first experiment (using RTTOV-5 and called thereafter CONTROL) was used as the control. The model first-guesses from the CONTROL experiment were then used together with the new RTTOV model to compute new observation departure statistics from which new satellite bias corrections were estimated (Harris and Kelly 2001). The second experiment, called RTTOV6M is identical to CONTROL apart from the use of RTTOV6M and the new bias correction files in the assimilation suite. Figure 6 represents the NOAA-14 HIRS-11 and HIRS-12 scan bias corrections required for the CONTROL experiment (left panel) and the RTTOV6M experiment (right panel). One can clearly see a decrease of the scan bias dependence, especially in the extra-tropics (red and green curves) for the RTTOV6M assimilation.

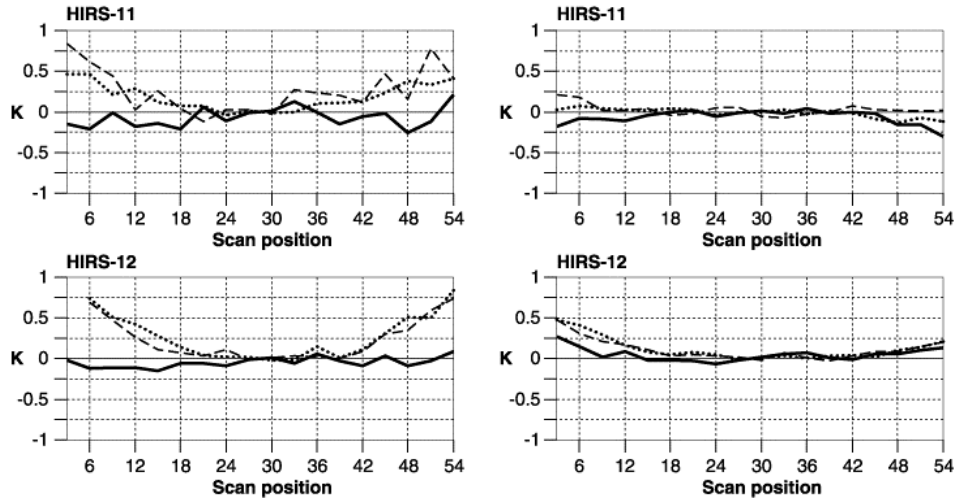

Figure 6. Scan bias correction for the channels HIRS-11 and HIRS-12 of NOAA-14 for the CONTROL experiment (left panel) and the RTTOV6M experiment (right panel). The solid curve denotes tropics, the dashed curve 50°S and the dotted curve 45°N-75°N.

Figure 7 represents the mean departure between uncorrected NOAA-14 HIRS-11 and 12 radiances and the model (solid curve), between bias corrected NOAA-14 HIRS-11 and 12 radiances and the model (dotted curve) as well as plus/minus one standard deviation of the corrected departure (dashed curve). These departures are plotted as a function of day. Left panel corresponds to the CONTROL experiment and right panel corresponds to RTTOV6M.

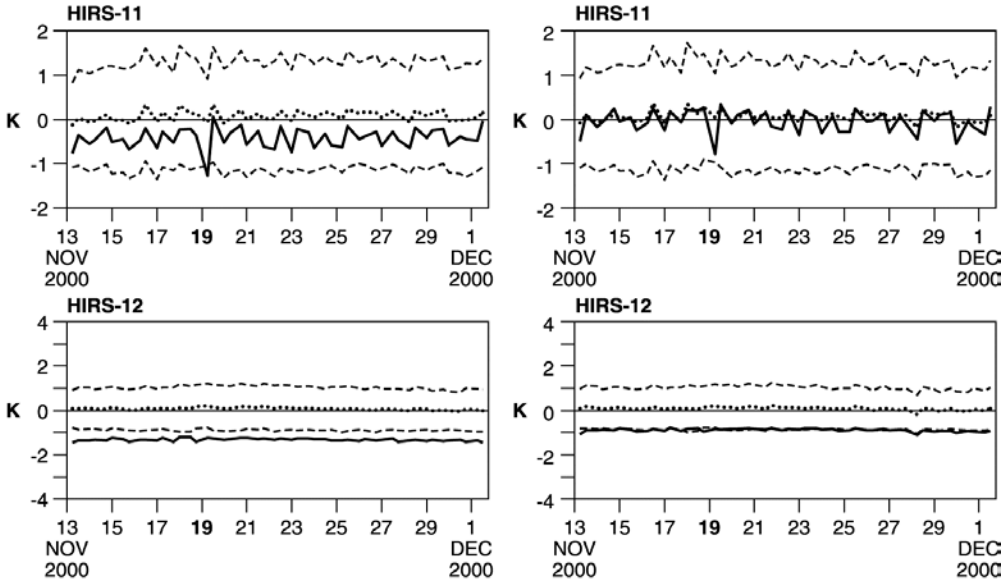

Figure 7. Mean value of the difference between measured and modelled radiances for the channels HIRS-11 and HIRS-12 of NOAA-14 for the CONTROL experiment (left panel) and RTTOV6M experiment (right panel). The solid curve denotes the uncorrected departure, the dotted curve the departure after bias correction and the dashed curve is plus/minus one standard deviation of the corrected departure.

The uncorrected curves show an improvement of the fit of the model to HIRS-11 and 12 radiances by .2 to 4K in the case of RTTOV6M, indicating a better general description of the upper tropospheric humidity in the model. In particular, the comparison to HIRS-11 (which is only used passively in the experiments) is particularly encouraging. Forecast scores have been accumulated over the three week period and turn out to

be neutral (not shown), which is not surprising bearing in mind the rather marginal use of the water vapour channels compared to all the other sources of information entering the assimilation system.

5. Conclusions

The set of predictors developed for RTIASI was implemented into the RTTOV-5 scheme in an effort to improve prediction of the HIRS channels. With the new predictors a closer fit to the LBL radiances is achieved for all the channels, the error being dramatically reduced for channel HIRS-8, HIRS-9, HIRS-10, HIRS-11 and, most significantly, HIRS-12. In particular, for the water vapour channels HIRS-11 and HIRS-12 a seven-fold reduction of the rms error was obtained. Comparison with LBL computed Jacobians show that Jacobians generated by the improved RTTOV-5 are remarkably close to the LBL ones. For most of the cases considered in the study the quality of the fit is at a level typical of LBL models. Conversely, Jacobians generated by the operational model differ from the LBL ones in amplitude and shape and to some degree the peak position. Comparison of the improved RTTOV-5 radiances with equivalent quantities computed using an independent LBL model for a large set of atmospheric profiles show that errors do not display any marked dependence on the air-mass type whereas for the operational model the warmer and moister the profile the larger the error. The RTTOV-5 with new predictors is also able to reproduce radiances for all the microwave sounders supported by RTTOV-5 to accuracy at or below the one achieved by use of dedicated predictors in the operational version of the model. This means that a single set of predictors can be used to accurately simulate radiances for a wide range of satellite instruments, from the conventional infrared to microwave sounders. As a result of this, a new version of RTTOV, RTTOV-7, has been jointly developed with Météo France and The Met Office that among the other new features includes the use of the new predictors.

Acknowledgements

The LBL computed Jacobians were provided by L. Garand (MSC, Canada). Roger Saunders (The Met Office, UK) provided the convolved transmittances for the HIRS channels. Synsatrad was provided by Stephen Tjemkes (EUMETSAT, Germany). Discussions with A. McNally, staff at ECMWF, were also valuable during the course of this work.

References:

Chevallier, F., Chedin, A., Cheruy, N., and Morcrette, J.J., "TIGR-like atmospheric profile database for accurate radiative flux computation, "*Q. J. R. Meteorol. Soc*., **126**, pp. 777-785.

Edwards, D.P., 1992, "GENLN2. A general line-by-line atmospheric transmittance and radiance model", NCAR Technical note NCAR/TN-367+STR.

ERA-40: ECMWF Re-Analysis, web site http://www.ecmwf..int/research/era

Eyre, J.R., 1991, "A fast radiative transfer model for satellite sounding system", ECMWF Research Department Technical memorandum 176 (European Centre for Medium-Range Weather Forecasts, Reading, UK).

Fortuin, J.P.F., and Langematz, U., "An update of the global ozone climatology and on current ozone and temperature trends," Proc. SPIE 2311, pp. 207-216 (1994).

Garand, L., Turner, D.S., Larocque, M., Bates, J., Boukabara, S., Brunel, P., Chevallier, F., Deblonde, G., Engelen, R., Hollingshead, M., Jackson, D., Kedlovec, G., Joiner, J., Kleespies, T., McKague, D.S., McMillin, L., Moncet, J.-L., Pardo, J.R., Rayer, P.J., Salathe, E., Saunders, R., Scott, N.A., Van Delst, P. and Woolf, H., 2001, "Radiance and jacobian intercomparison of radiative transfer models applied to HIRS and AMSU channels", in print, J. Geophys. Res., **106**, 15 pp.

Hannon, S.E., Strow, L.L. and McMillan, W.W., 1996, "Atmospheric infrared fast transmittance models: a comparison of two approaches", *in Optical Spectroscopic Techniques and Instrumentation for Atmospheric and Space Research II*, P.B. Hays and J. Wang, eds., Proc. SPIE **2830**, pp. 94-105.

Harris, B.A. and Kelly, G., 2001," A satellite radiance-bias correction scheme for data assimilation", *Q. J. R. Meteorol. Soc*., **127**, pp. 1453-1468.

Matricardi, M. and Saunders, R., 1999, "Fast radiative transfer model for simulation of infrared atmospheric sounding interferometer radiances", *Applied Optics*, **38**, pp. 5679-5691.

Matricardi, M., Chevallier, F. and Tjemkes, S., 2001, "An improved general fast radiative transfer model for the assimilation of radiance observations", ECMWF Research Department Technical memorandum 345 (European Centre for Medium-Range Weather Forecasts, Reading, UK).

Fleming, H.E. and McMillin, L., 1977, "Atmospheric transmittance of an absorbing gas. 2. A computationally fast and accurate transmittance model for slant paths at different zenith angles", *Appl. Opt*., **16**, pp. 1366-1370.

McMillin, L.M., Fleming, H.E. and Hill, M.L., 1979, "Atmospheric transmittance of an absorbing gas. 3: A computationally fast and accurate transmittance model for absorbing gases with variable mixing ratios", *Appl. Opt*., **18**, pp. 1600-1606.

Rabier, F., ThJpaut, J. and Courtier, P., 1998, "Extended assimilation and forecast experiments with a four dimensional variational assimilation scheme", *Q. J. R. Meteorol. Soc*., **124**, pp. 1861-1887.

Rizzi, R., Matricardi, M. and Miskolczi, F., 2001, "On the simulation of up-looking and down-looking high-resolution radiance spectra using two different radiative transfer models", Accepted for publication in *Applied Optics.*

Saunders, R., Matricardi, M. and Brunel, P., 1999, "A fast radiative transfer model for assimilation of satellite radiance observations – RTTOV-5", *ECMWF Research Department Technical Memorandum 282 (European Centre for Medium-Range Weather Forcasts, Reading, UK, 1999*

Sneden, C, Johnson, H. and Krupp, B., 1975, "A statistical method for trating molecular line opacities", *Astrophys. J*., **204**, pp. 281-289.

Susskind, J., Rosenfeld, J. and Reuter, D., 1983, "An accurate radiative transfer model for use in the direct physical inversion of HIRS2 and MSU temperature sounding data", *J. Geophys. Res*., **88**, pp.8850-8568.

Tjemkes, S.A. and Schmetz, J., 1997, "Synthetic satellite radiances using the radiance sampling method", *J. Geophys. Res*., **102D**, pp. 1807-1818.